Bio-Design and Manufacturing (2024) 7:591–595
https://doi.org/10.1007/s42242-024-00283-5

LETTER

Implantable probe with integrated reference electrode for in situ neural signal and calcium ion monitoring

Junyu Xiao[1,2] · Mengfei Xu[1,2] · Longchun Wang[1,2] · Bin Yang[1] · Jingquan Liu[1]

Received: 2 October 2023 / Accepted: 27 April 2024 / Published online: 1 July 2024

Monitoring the electrophysiology activity of neurons and blood calcium signals can enable a better understanding of disease-related neural system circuits. However, currently, in situ calcium ion monitoring tools are scarce and exhibit low integration and limited sensitivity. In this letter, we propose an implantable probe with an integrated in situ Ag/AgCl reference electrode (ISA/ARE) that can monitor action potential (AP) and Ca^{2+} concentrations. The experimental results indicate that the sensitivity of Ca^{2+} sensors can reach 100.7 mV/decade and their selectivity is excellent in the presence of interference. The AP of neurons was recorded using 12 electrophysiology microelectrodes modified with platinum black, while their reversible potential changes could be observed with the Ca^{2+} sensor when $CaCl_2$ solutions were repeatedly microinjected into specific regions of the brain. These results demonstrate that the probe can satisfy the requirements for synchronous monitoring of electrophysiology signals and ion concentrations for further understanding neural circuits, thereby promoting the development of brain science.

Introduction

Neuroscience has always been committed to decoding brain information, helping clinicians to identify the root causes of many neurological and mental disorders [1–3]. Various efforts to decipher brain information led to the emergence of tools, such as silicon neural probes, which can record high-spatiotemporal-resolution brain activity [4–7]. Although the number of electrodes for electrophysiology recording has been increased considerably, the drawback of most neural probes is that they can only record a single type of neural signal.

In addition to electrophysiology signals, brain sends out numerous biochemical signals, such as those corresponding to Ca^{2+}, K^+, Na^+, Mg^{2+}, and neurotransmitters [8–10]. The main function of Ca^{2+} in the blood is to stabilize neurons and prevent abnormal discharge activity of membrane potential; therefore, Ca^{2+} can effectively inhibit neural system diseases such as seizures [11]. However, implanted Ca^{2+} imaging devices generally exhibit poor resolution, necessitate high surgical requirements, and cause substantial postoperative damage [12, 13]. Therefore, the development of high-resolution Ca^{2+} sensors that can be easily implanted in the brain is urgently required.

This study presents an implantable probe with an ISA/ARE for monitoring AP and Ca^{2+} concentrations in the brain. The sensitivity of Ca^{2+} sensors reaches up to 100.7 mV/decade, which is three times that of existing Ca^{2+} sensors [14]. The experimental results from in vitro and in vivo investigations demonstrated the capability of the implantable probe to sense a 12-channel biopotential and Ca^{2+} concentrations in specific regions. The Ca^{2+} sensors can be further optimized to achieve higher spatial resolution and promote brain–computer interface [15] and cross-species communication [16].

Probe preparation

The schematics and concept of the probe implanted in the brain area of a mouse are outlined in Fig. 1a. The shanks can be implanted into specific brain regions of the mouse while monitoring its neural responses, such as AP and ion concentrations. Micro-electrical–mechanical system technology was used to manufacture the implantable probes in a high-throughput manner (Fig. 1b). The developed four-inch silicon wafer with 68 probes is shown in Fig. 1c.

✉ Jingquan Liu
jqliu@sjtu.edu.cn

1 National Key Laboratory of Advanced Micro and Nano Manufacture Technology, Shanghai Jiao Tong University, Shanghai 200240, China

2 Department of Micro/Nano Electronics, Shanghai Jiao Tong University, Shanghai 200240, China

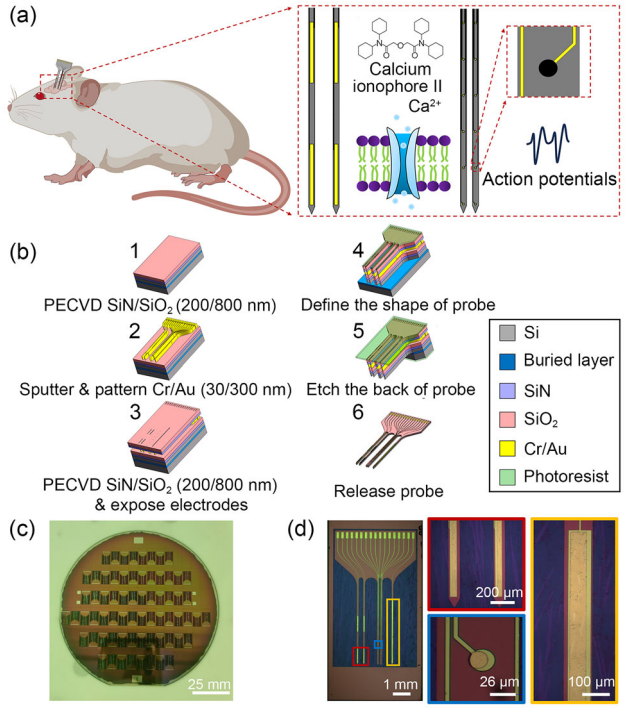

Fig. 1 **a** Design of the probe and its application in a mouse. **b** Fabrication processes. **c** Photograph of the wafer. **d** Ultra-depth-field images of a single probe. PECVD: plasma-enhanced chemical vapor deposition

A single probe on a wafer was characterized using an ultra-depth-field microscope (Fig. 1d). The shanks could carry different electrodes. The two shanks on the left side of the probe contain four working electrodes for ion sensing (red wireframe), middle two shanks contain 12 circular microelectrodes for electrophysiology recording (blue wireframe), and the rightmost shank contains a rectangular electrode that acts as an in situ reference electrode (yellow wireframe). The four working electrodes (60 μm× 1000 μm) used for the preparation of Ca^{2+} sensors can be coated with poly(3,4-ethylenedioxythiophene): polystyrene sulfonate (PEDOT:PSS) to realize ion-to-electron transduction and modification with Ca^{2+} selective membranes. The 12 circular microelectrodes for electrophysiology recording (diameter: 26 μm) were modified with platinum black to reduce contact impedance during the measurement. The rectangular electrode (60 μm×3980 μm) was made into an ISA/ARE via the constant current method.

Electrode modification

Electrophysiology recording microelectrodes

The cyclic voltammetry curve of the platinum black electrode exhibits a highly faradic behavior corresponding to a much larger elliptical shape than that of the bare electrode (Fig. 2a), indicating its improved charge storage capacity and transfer. Compared with the bare electrode, the impedance of the platinum black electrode at 1 kHz decreases by 86%, enhancing the fidelity of the neural signal recording (Fig. 2b) [17]. The ultra-depth-field (Fig. 2c) and scanning electron microscopy images (Fig. 2d) verify the successful modification of the platinum black electrode.

In situ Ag/AgCl reference electrode

The constant current method is used to prepare the ISA/ARE [18, 19]. First, the reference electrode is set as the cathode, and a Ag foil is set as the working electrode; furthermore, a current density of 10 mA/cm^2 is applied to them for 20 min. During the electroplating process, the surface potential of the reference electrode remains stable at around 1.1 V (Fig. 3a), and the ultrasonic water bath method ensures the uniform distribution of Ag^+ in the solution. Second, the reference electrode is set as the working electrode and applied with a current density of 0.4 mA/cm^2 for 10 min. The platinum electrode is set as the counter electrode in 1 mol/L KCl solution. Figure 3b shows that the chlorination voltage is around 1.4 V. Figure 3c shows the energy-dispersive X-ray spectroscopy (EDS) layered images of the elements on the ISA/ARE, where the Ag is shown in red, Cl shown in blue, and Au shown in green. The atomic percentages of these three elements are as follows: 52.35% of Ag, 47.36% of Cl, and 0.28% of Au (Fig. 3d).

Results and discussion

In vitro experiments

The preparation of the Ca^{2+} ion-selective sensor is shown in Fig. 4a. The electrode surface was coated with a layer of PEDOT:PSS for ion–electron conduction, followed by a layer of calcium ion-selective solution, and was dried overnight to form a thin film [20–22]. The Ca^{2+} sensor was characterized in a $CaCl_2$ electrolyte solution and exhibited a linear response with increasing Ca^{2+} concentration, the sensitivity of which is 100.7 mV/decade (Fig. 4b). Additionally, the thin film morphology on the Ca^{2+} sensor surface is shown in Fig. 4b. To determine the selectivity of Ca^{2+} sensors, interfering analytes (such as Mg^{2+}, K^+, and Na^+) were added in a $CaCl_2$ electrolyte solution (1 mmol/L). The results in Fig. 4c show that Ca^{2+} sensors continue to exhibit excellent selectivity toward the target electrolyte even in the presence of other interference. Four different Ca^{2+} sensors were used for experiments to determine the variations in sensors owing to manufacturing errors. The sensitivity range of the Ca^{2+} sensor is 80.4–102.8 mV/decade, with a relative standard deviation of 13.43% (Fig. 4d). The characterization results

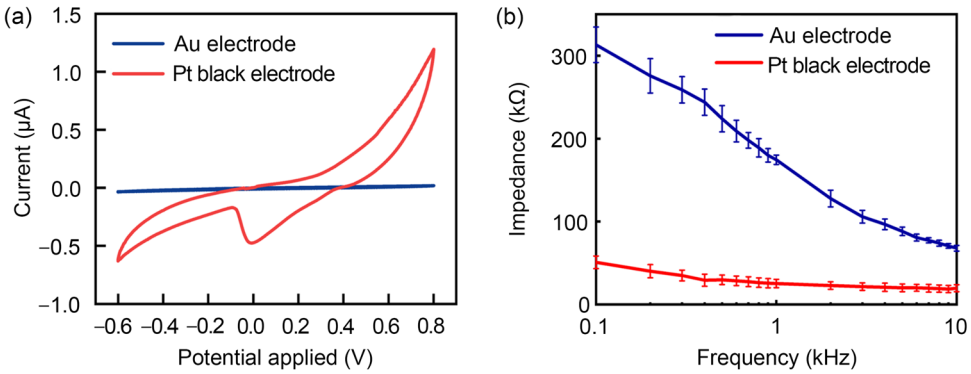

Fig. 2 **a** Cyclic voltammetry curves before and after the modification with platinum black. **b** Impedance (data are expressed as mean±standard deviation, n=3), **c** ultra-depth-field images, and **d** scanning electron microscopy images of microelectrodes

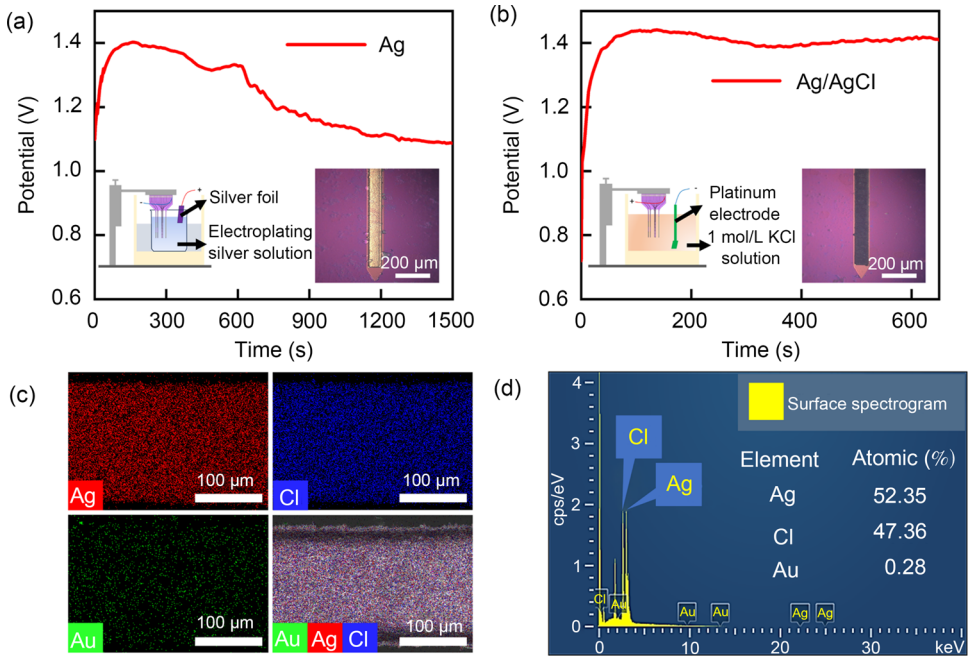

Fig. 3 Voltage curves for **a** electroplating silver layer and **b** chlorinating Ag layer. **c** Energy-dispersive X-ray spectroscopy (EDS) layered images and **d** surface spectrogram of integrated in situ Ag/AgCl reference electrode (ISA/ARE)

of the Ca^{2+} sensor indicate that it has high sensitivity and selectivity for chemical detection.

In vivo experiments

The probe is demonstrated to be capable of 12-channel electrophysiology recording of neural activity. The probe was implemented into the CA1 region of the brain (Fig. 5a), and a local field potential (LFP) reflecting the dynamic flow of neuronal information in the brain was obtained (Fig. 5b). The LFP signal is mainly concentrated at low frequencies (<300 Hz), while the spontaneous spike signal is concentrated at high frequencies (>300 Hz) [23, 24]. By performing high-pass filtering on raw signals above 300 Hz and using principal component analysis for classification of spikes (Fig. 5c), spontaneous spike signals could be obtained. The

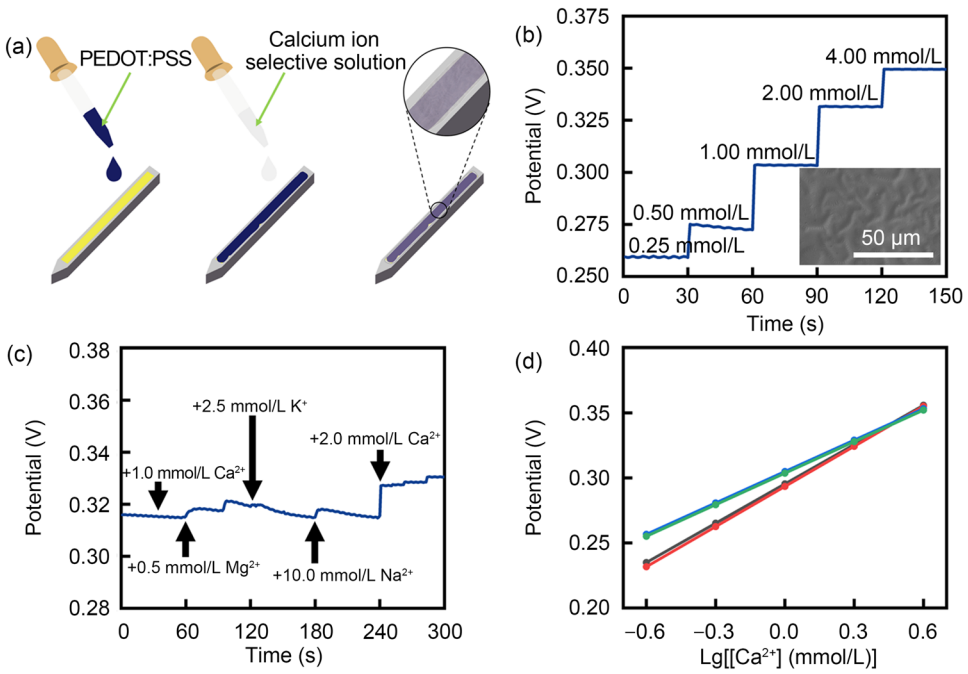

Fig. 4 **a** Preparation of Ca^{2+} sensor. **b** Open circuit potential response of the Ca^{2+} sensor in $CaCl_2$ solution. **c** Selectivity of the Ca^{2+} sensors. **d** Differences in sensor responses between the four Ca^{2+} sensors (different colors denote different sensors). PEDOT:PSS: poly(3, 4-ethylenedioxythiophene): polystyrene sulfonate

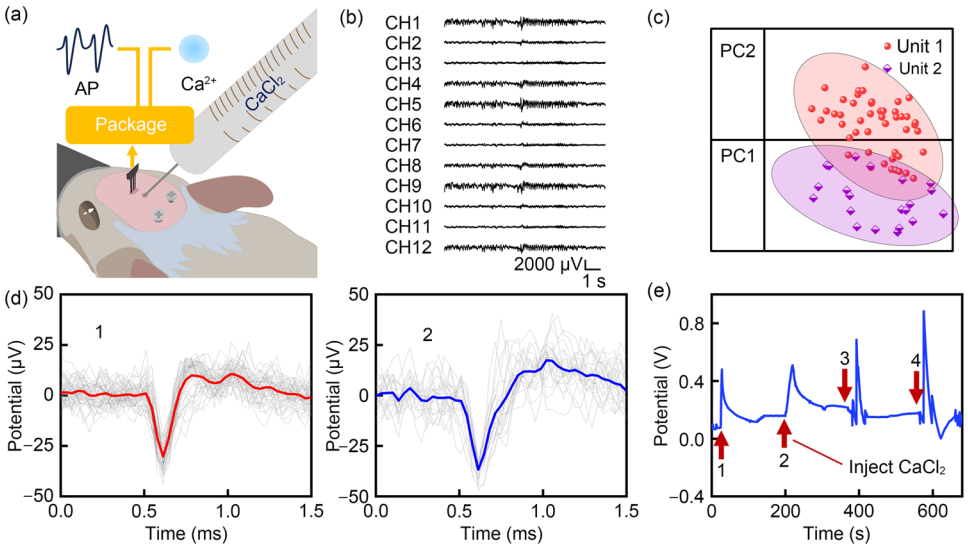

Fig. 5 **a** Schematic of in vivo experiments. **b** Twelve-channel local field potential (LFP) data (10 s) recorded from CA1. **c** Principal component analysis for classification of spikes. **d** Spontaneous extracellular spikes from CA1. **e** Cyclic potentials of the Ca^{2+} sensor during the repeated microinjection process. AP: action potential; PC1: principal component 1; PC2: principal component 2

results indicated that the neurons may produce two different spikes (Fig. 5d). These results demonstrate that the probe can map spontaneous neural activity in specific brain regions.

We injected 10 μL of $CaCl_2$ solution (1 mmol/L) at 2 mm from the probe implantation point (Fig. 5a). When injection was repeated, the Ca^{2+} sensor on the probe exhibited reversible potential changes (Fig. 5e). A significant potential peak was generated due to an increase in Ca^{2+} concentration in the tissue fluid of the region. The recovery of potential may be attributed to the self-regulation ability of the extracellular environment. In the first two cyclic potentials, 10 μL of $CaCl_2$ solution was injected into the brain area at a uniform rate within 8 s, demonstrating a peak potential of 0.4 V and a recovery time of 100 s. In the last two cyclic potentials, 10 μL of $CaCl_2$ solution was injected into the brain area within 4 s, yielding a peak potential of 0.8 V and recovery time of 50 s. Therefore, there may be a correlation between injection speed, potential amplitude, and potential recovery time. The results obtained indicate that this probe provides a new method for evaluating the effectiveness of neural regulation.

The AP measurements and calcium ion sensing were performed independently. In the future, we intend to stimulate neurons to spontaneously change the concentration of intracellular and extracellular calcium ions through drugs or external optics. This will help us to simultaneously record AP and Ca^{2+} sensing potential.

Conclusions

In summary, this work presents an implantable probe with ISA/ARE. Notably, in vitro and in vivo experimental results demonstrate the capability of the implantable probe to sense a 12-channel biopotential and Ca^{2+} concentrations in specific regions of the brain. The newly developed probe can help explore the mechanisms of various neurological diseases.

Acknowledgements This work was supported by the STI 2030—Major Projects (Nos. 2022ZD0208601 and 2022ZD0208600), the National Key R&D Program of China (Nos. 2022YFF120301 and 2020YFB1313502), the Fundamental Research Funds for the Central Universities, the Strategic Priority Research Program of Chinese Academy of Sciences (Nos. XDA25040100, XDA25040200, and XDA25040300), the National Natural Science Foundation of China (No. 42127807-03), the Shanghai Municipal Science and Technology Major Project (No. 2021SHZDZX), and China Postdoctoral Science Foundation (No. 2023M732197). The authors are also grateful to the Center for Advanced Electronic Materials and Devices (AEMD) of Shanghai Jiao Tong University, China.

Author contributions JYX conducted the study and wrote the original draft; MFX helped in supervision and writing—review and editing; LCW contributed to conceptualization and methodology; BY and JQL supervised the study.

Declarations

Conflict of interest All the authors declare that they have no conflict of interest.

Ethical approval All institutional and national guidelines for the care and use of laboratory animals were followed. In vivo experiments were conducted in accordance with the Chinese Animal Experimentation Law and approved by the Experimental Animal Ethics and Use Committee of Shanghai Jiao Tong University (approval number: 202301135).

References

1. Alivisatos AP, Andrews AM, Boyden ES et al (2013) Nanotools for neuroscience and brain activity mapping. ACS Nano 7(3):1850–1866. https://doi.org/10.1021/nn4012847
2. Altieri SC, Yang HY, O'Brien HJ et al (2015) Perinatal vs genetic programming of serotonin states associated with anxiety. Neuropsychopharmacology 40(6):1456–1470. https://doi.org/10.1038/npp.2014.331
3. Topalovic U, Aghajan ZM, Villaroman D et al (2020) Wireless programmable recording and stimulation of deep brain activity in freely moving humans. Neuron 108(2):322–334.e9. https://doi.org/10.1016/j.neuron.2020.08.021
4. Raducanu BC, Yazicioglu RF, Lopez CM et al (2017) Time multiplexed active neural probe with 1356 parallel recording sites. Sensors 17(10):2388–2408. https://doi.org/10.3390/s17102388
5. Jun JJ, Steinmetz NA, Siegle JH et al (2017) Fully integrated silicon probes for high-density recording of neural activity. Nature 551(7679):232–236. https://doi.org/10.1038/nature24636
6. Steinmetz NA, Aydin C, Lebedeva A et al (2021) Neuropixels 2.0: a miniaturized high-density probe for stable, long-term brain recordings. Science 372(6539):eabf4588. https://doi.org/10.1126/science.abf4588
7. Musk E, Neuralink (2019) An integrated brain-machine interface platform with thousands of channels. J Med Internet Res 21(10):e16194. https://doi.org/10.2196/16194
8. Aroonyadet N, Wang XL, Song Y et al (2015) Highly scalable, uniform, and sensitive biosensors based on top-down indium oxide nanoribbons and electronic enzyme-linked immunosorbent assay. Nano Lett 15(3):1943–1951. https://doi.org/10.1021/nl5047889
9. Liu QZ, Zhao CZ, Chen MR et al (2020) Flexible multiplexed In_2O_3 nanoribbon aptamer-field-effect transistors for biosensing. iScience 23(9):101469. https://doi.org/10.1016/j.isci.2020.101469
10. Nakatsuka N, Yang KA, Abendroth JM et al (2018) Aptamer–field-effect transistors overcome Debye length limitations for small-molecule sensing. Science 362(6412):319–324. https://doi.org/10.1126/science.aao6750
11. Huang WJ, Ke Y, Zhu JP et al (2021) TRESK channel contributes to depolarization-induced shunting inhibition and modulates epileptic seizures. Cell Rep 36(3):109404. https://doi.org/10.1016/j.celrep.2021.109404
12. Ouzounov DG, Wang TY, Wang MR et al (2017) In vivo three-photon imaging of activity of GCaMP6-labeled neurons deep in intact mouse brain. Nat Methods 14(4):388–390. https://doi.org/10.1038/nmeth.4183
13. Yang WJ, Yuste R (2017) In vivo imaging of neural activity. Nat Methods 14(4):349–359. https://doi.org/10.1038/nmeth.4230
14. Ling W, Yu JX, Ma N et al (2020) Flexible electronics and materials for synchronized stimulation and monitoring in multi-encephalic regions. Adv Funct Mater 30(32):2002644. https://doi.org/10.1002/adfm.202002644
15. Niederkofler V, Asher TE, Dymecki SM (2015) Functional interplay between dopaminergic and serotonergic neuronal systems during development and adulthood. ACS Chem Neurosci 6(7):1055–1070. https://doi.org/10.1021/acschemneuro.5b00021
16. Vaiana M, Muldoon SF (2020) Multilayer brain networks. J Nonlinear Sci 30(5):2147–2169. https://doi.org/10.1007/s00332-017-9436-8
17. Abbott J, Ye TY, Krenek K et al (2020) A nanoelectrode array for obtaining intracellular recordings from thousands of connected neurons. Nat Biomed Eng 4(2):232–241. https://doi.org/10.1038/s41551-019-0455-7
18. Brewer PJ, Leese RJ, Brown RJC (2012) An improved approach for fabricating Ag/AgCl reference electrodes. Electrochim Acta 71:252–257. https://doi.org/10.1016/j.electacta.2012.03.164
19. Tjon KCE, Yuan J (2019) Impedance characterization of silver/silver chloride micro-electrodes for bio-sensing applications. Electrochim Acta 320:134638. https://doi.org/10.1016/j.electacta.2019.134638
20. Lee YK, Jang KI, Ma Y et al (2017) Chemical sensing systems that utilize soft electronics on thin elastomeric substrates with open cellular designs. Adv Funct Mater 27(9):1605476. https://doi.org/10.1002/adfm.201605476
21. Nyein HYY, Gao W, Shahpar Z et al (2016) A wearable electrochemical platform for noninvasive simultaneous monitoring of Ca^{2+} and pH. ACS Nano 10(7):7216–7224. https://doi.org/10.1021/acsnano.6b04005
22. Parrilla M, Cuartero M, Crespo GA (2019) Wearable potentiometric ion sensors. TrAC Trends Anal Chem 110:303–320. https://doi.org/10.1016/j.trac.2018.11.024
23. Lausen T, Keil S, Thewes R (2023) An ultra low power pixel for implantable neural interfaces. In: 9th International Workshop on Advances in Sensors and Interfaces, p.325–328. https://doi.org/10.1109/IWASI58316.2023.10164384
24. Prasad A, Sahin M (2009) Spinal cord recordings in rats during skilled reaching task. Annual International Conference of the IEEE Engineering in Medicine and Biology Society, p.582–585. https://doi.org/10.1109/IEMBS.2009.5332818